Intramolecular Electron Transfer in Mixed-Valence Biferrocenium Salts Containing Heteroatoms: Preparation, Structure, and ^{57}Fe Mössbauer Characteristics

Teng-Yuan Dong,*[,1] Chung-Kay Chang,[1] Shu-Hwei Lee,[1] Long-Li Lai,[1] Michael Yen-Nan Chiang,[1] and Kuan-Jiuh Lin[2]

Department of Chemistry, National Sun Yat-Sen University, Kaohsiung, Taiwan, and the Institute of Chemistry, Academia Sinica, Nankang, Taipei, Taiwan

Received August 20, 1997[⊗]

A convenient new method is developed for the preparation of 1′,1‴-disubstituted biferrocenes which can be oxidized with iodine to a new series of mixed-valence compounds. The X-ray structures of 1′,1‴-dimethoxymethyl, 1′,1‴-diethoxyl, 1′,1‴-dimethyl, 1′,1‴-dihydroxymethyl, 1′,1‴-dibenzoyloxymethyl, 1′,1‴-dimethylthio, and 1′,1‴-diethylthio neutral biferrocenes and the mixed-valence 1′,1‴-diethoxyl, 1′,1‴-dimethyl, 1′,1‴-dibenzoyloxymethyl, and 1′,1‴-diphenylthio biferrocenium triiodide salts have been determined at 298 K. The rates of intramolecular electron transfer in these mixed-valence cations were estimated by variable-temperature ^{57}Fe Mössbauer experiment.

Introduction

The study of intramolecular electron transfer in mixed-valence complexes has enabled systematic and creative investigation into the factors that affect rates of electron transfer in solution redox processes, solid-state materials, and biological electron-transfer chain.[3−6] In the case of mixed-valence 1′,1‴-disubstituted biferrocenium triiodide salts (**1**; Chart 1), considerable progress has been made in understanding the factors that control the rate of intramolecular electron transfer in the solid state.[7−19] In the series of mixed-valence biferrocenium cations (**1**), the rate of electron transfer is influenced by various structural factors and lattice dynamics,[7−11] including the electronic and vibronic coupling between two metal ions,[12−15] the nature of the counterion,[16−18] and cation−anion interactions.[19] However, owing to the methodological limitation in the preparation of the neutral 1′,1‴-disubstituted biferrocene, not many biferrocenium triiodide salts have been obtained for electron-transfer studies and the substituents on the 1′,1‴ position were mostly simple alkyl groups, halide, or benzyl derivatives. No biferrocenium triiodide salt containing heteroatoms or a heterocyclic ring has ever been prepared.

Chart 1

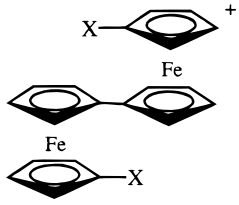

1a X = H **1e** X = $CH_2C_6H_5$
1b X = C_2H_5 **1f** X = I
1c X = C_3H_7 **1g** X = Br
1d X = C_4H_9 **1h** X = Cl

To study the influence of the electronic effects of the substituent on the cyclopentadienyl (Cp) ring, we have prepared a new series of 1′,1‴-heterosubstituted biferrocene and their corresponding biferrocenium triiodide salts. We now show that there is a dramatic difference in the electron-transfer rate for this new series of biferrocenium salts. Furthermore, the preparation and electrochemical measurements for neutral biferrocene compounds are also presented.

Results and Discussion

Methodology. We attempted to develop an alternative method to synthesize 1′,1‴-dibromobiferrocene, which is an important precursor of 1′,1‴-disubstituted biferrocenes. A compound of 1′,1‴-dibromobiferrocene was previously prepared by the direct bromination of ferrocene.[20] Noteworthy is that 1′,1‴-dibromobiferrocene is the minor product and the yield is quite low

[⊗] Abstract published in *Advance ACS Abstracts,* November 15, 1997.

(1) National Sun Yat-Sen University.
(2) Academia Sinica.
(3) Day, P. *Int. Rev. Phys. Chem.* **1981**, *1*, 149.
(4) Brown, D. *Mixed-Valence Compounds, Theory and Applications in Chemistry, Phyiscs, Geology and Biology*; Reidel: Boston, MA, 1980.
(5) Creutz, C. *Prog. Inorg. Chem.* **1983**, *30*, 1.
(6) Richardson, D. E.; Taube, H. *Coord. Chem. Rev.* **1984**, *60*, 107.
(7) Cohn, M. J.; Dong, T.-Y.; Hendrickson, D. N.; Geib, S. J.; Rheingold, A. L. *J. Chem. Soc., Chem. Commun.* **1985**, 1095.
(8) Dong, T.-Y.; Hendrickson, D. N.; Iwai, K.; Cohn, M. J.; Rheingold, A. L.; Sano, H.; Motoyama, S. *J. Am. Chem. Soc.* **1985**, *107*, 7996.
(9) Iijima, S.; Saida, R.; Motoyama, I.; Sano, H. *Bull. Chem. Soc. Jpn.* **1981**, *54*, 1375.
(10) Nakashima, S.; Katada, M.; Motoyama, I.; Sano, H. *Bull. Chem. Soc. Jpn.* 1**987**, *60*, 2253.
(11) Kai, M.; Katada, M.; Sano, H. *Chem. Lett.* **1988**, 1523.
(12) Dong, T.-Y.; Lee, T. Y.; Lee, S. H.; Lee, G. H.; Peng, S. M. *Organometallics* **1994**, *13*, 2337.
(13) Dong, T.-Y.; Ke, T. J.; Peng, S. M.; Yeh, S. K. *Inorg. Chem.* **1989**, *28*, 2103.
(14) Dong, T.-Y.; Hwang, M. Y.; Wen, Y. S. *J. Organomet. Chem.* **1990**, *391*, 377.
(15) Dong, T.-Y.; Lee, T. Y.; Lin, H. M. *J. Organomet. Chem.* **1992**, *427*, 101.
(16) Dong, T.-Y.; Schei, C. C.; Hsu, T. L.; Lee, S. L.; Li, S. J. *Inorg. Chem.* **1991**, *30*, 2457.
(17) Webb, R. J.; Geib, S. J.; Staley, D. L.; Rheingold, A. L.; Hendrickson, D. N. *J. Am. Chem. Soc.* **1990**, *112*, 5031.
(18) Dong, T.-Y.; Kambara, T.; Hendrickson, D. N. *J. Am. Chem. Soc.* **1986**, *108*, 5857.
(19) Kambara, T.; Hendrickson, D. N.; Dong, T.-Y.; Cohn, M. J. *J. Chem. Phys.* **1987**, *86*, 2362.
(20) Kovar, R. F.; Rausch, M. D.; Rosenberg, H. *Organomet. Chem. Synth.* **1971**, *1*, 173.

S0276-7333(97)00746-2 CCC: $14.00

Scheme 1

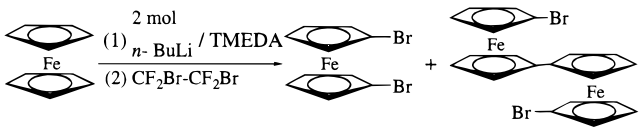

Table 1. Experimental and Crystal Data for the X-ray Structures of Neutral Biferrocenes

	4	**6**	**8**
formula	$C_{24}H_{26}Fe_2O_2$	$C_{24}H_{26}Fe_2O_2$	$C_{22}H_{22}Fe_2$
mol wt	458.16	458.16	398.11
cryst syst	orthorhombic	monoclinic	tetragonal
space group	$P2_12_12_1$	$P2_1/n$	$P4_12_12$
a, Å	7.486(4)	7.528(1)	7.604(2)
b, Å	16.430(4)	14.682(1)	
c, Å	16.331(4)	18.423(2)	29.503(4)
β, deg	97.36		
ρ_{calcd}, g cm^{-3}	1.515	1.507	1.550
V, Å^3	2008.5(12)	2019.6(4)	1705.8(7)
Z	4	4	4
μ, mm^{-1}	1.44	1.45	1.698
λ, Å	0.710 69	0.710 69	0.710 69
2θ limits, deg	49.9	44.9	50.0
R_f[a]	0.032	0.031	0.037
R_{wf}[b]	0.033	0.034	0.042

[a] $R_f = \sum(||F_o| - |F_c||)/\sum|F_o|$. [b] $R_{wf} = \sum[(w(Fo - F_c)^2)/\sum(wF_o^2)]^{1/2}$.

(4%, Scheme 1). We have found that 1′,1‴-dibromobiferrocene can be prepared easily by direct coupling of 1,1′-dibromoferrocene, using CuCN and oxygen as the coupling reagent (Scheme 2). The yield was maintained at 50% after work-up and recrystallization. Reaction of 1′,1‴-dibromobiferrocene with 2 equiv of butyllithium in dry THF led to 1′,1‴-dithiobiferrocene. The crude 1′,1‴-dilithiobiferrocene without being isolated was in situ treated with various electrophilic reagents, and the Cp rings were, thus, functionalized with various substituents (Scheme 3).

In our previous paper,[21,22] we reported a general procedure to prepare 1′-substituted 1-bromoferrocene by using the 1,1′-dibromoferrocene as a precursor. In the past, 1′,1‴-disubstituted biferrocenes, for example neutral compounds of **1a**−**e**, were prepared from the corresponding 1′-substituted 1-bromoferrocene, which was prepared by the acylation of bromoferrocene in the presence of $AlCl_3$ followed by reduction.[4] We found that the monolithioferrocene can be prepared easily and conveniently by adding stoichiometric amounts of *n*-BuLi to a THF solution of 1,1′-dibromoferrocene. Crude monolithioferrocene obtained in this way can be used in further electrophilic substitution reactions. Our method replaces the traditional Fridel−Crafts reaction for preparing bromoferrocene derivatives. As shown in Scheme 2, biferrocene **4** is synthesized by this alternative method.

Molecular Structures of Neutral Biferrocenes (4, 6, 8, 10, 11, and 14). Details of the X-ray crystal data collections and unit-cell parameters of neutral biferrocenes are given in Tables 1 and 2. Bond distances and angles are given as supporting information. The molecular structures of this series of neutral biferrocenes are also given as Supporting Information. A representative ORTEP drawing for **4** is shown in Figure 1. These neutral compounds exist in a trans conformation with the two iron ions on opposite sides of the planar fulvalenide moiety observed for most biferrocenes. The two Cp rings in the fulvalenide moiety are crystallographically coplanar for compounds **8**, **11**, **14a**, and **14b**. In the case of **4**, **6**, and **10**, the dihedral angles between the two Cp rings in the fulvalenide moiety are 2.1(3)°, 3.9(2)°, and 1.6(2)°, respectively. In these compounds, the substituents are located at the position above the ring of the other sandwich, as seen in other dialkyl biferrocenes.

Table 2. Experimental and Crystal Data for the X-ray Structures of Neutral Biferrocenes

	10	**11**	**14a**	**14b**
formula	$C_{22}H_{22}Fe_2O_2$	$C_{36}H_{30}Fe_2O_4$	$C_{22}H_{22}Fe_2S_2$	$C_{24}H_{26}Fe_2S_2$
mol wt	430.11	638.32	462.22	490.27
cryst syst	monoclinic	triclinic	monoclinic	triclinic
space group	$P2_1/c$	$P\bar{1}$	$P2_1/n$	$P\bar{1}$
a, Å	14.669(2)	5.816(2)	8.372(2)	7.300(2)
b, Å	7.776(2)	8.355(1)	12.659(3)	12.226(4)
c, Å	15.627(3)	14.696(2)	9.403(2)	12.525(5)
α, deg		79.87(1)		101.25(3)
β, deg	99.71(1)	87.83(2)	101.85(3)	95.00(3)
γ, deg		86.58(2)		90.88(2)
ρ_{calcd}, g cm^{-3}	1.626	1.511	1.574	1.491
V, Å^3	1757.1(5)	701.4(3)	975.3(4)	1091.7(6)
Z	4	1	2	2
μ, mm^{-1}	1.66	1.07	1.704	1.527
λ, Å	0.710 69	0.710 69	0.710 69	0.710 69
2θ limits, deg	45.0	44.9	44.98	44.86
R_f[a]	0.028	0.034	0.027	0.038
R_{wf}[b]	0.036	0.035		
wR2[c]			0.090	0.098

[a] $R_f = \sum(||F_o| - |F_c||)/\sum|F_o|$. [b] $R_{wf} = \sum[(w(F_o - F_c)^2)/\sum(wF_o^2)]^{1/2}$. [c] $wR2 = [(\sum w(F_o^2 - F_c^2)^2)/(\sum wF_o^2)^2]^{1/2}$, where $w = 1/[\sigma^2(F_o^2) + (fp)^2]$, $p = (\max(F_o^2; 0) + 2F_c^2)/3$, and $f = 0.1000$ for **14a** and 0.1626 for **14b**.

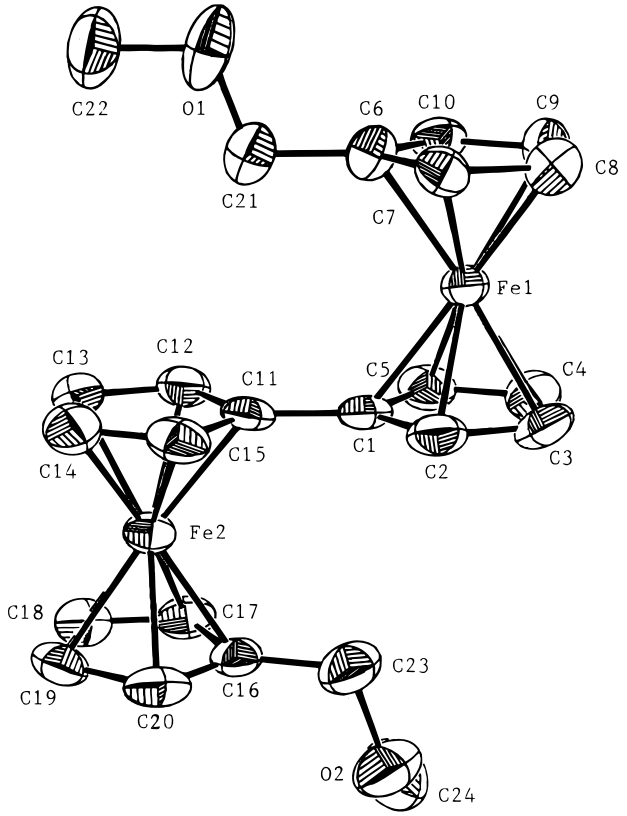

Figure 1. ORTEP drawing of **4**.

(21) Lai, L. L.; Dong, T.-Y. *J. Chem. Soc., Chem. Commun.* **1994**, 2347.
(22) Dong, T.-Y.; Lai, L. L. *J. Organomet. Chem.* **1996**, *509*, 131.

Scheme 2

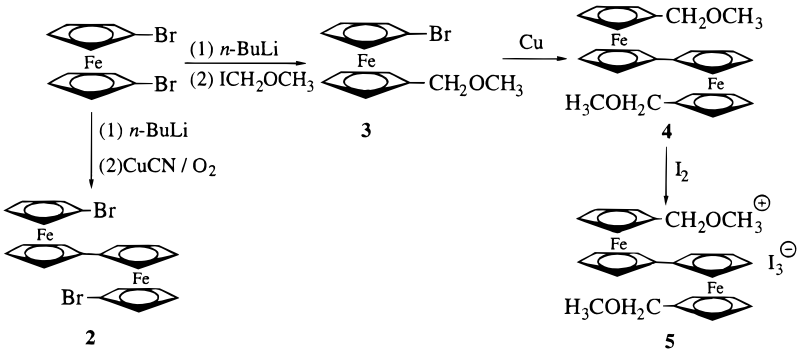

Scheme 3

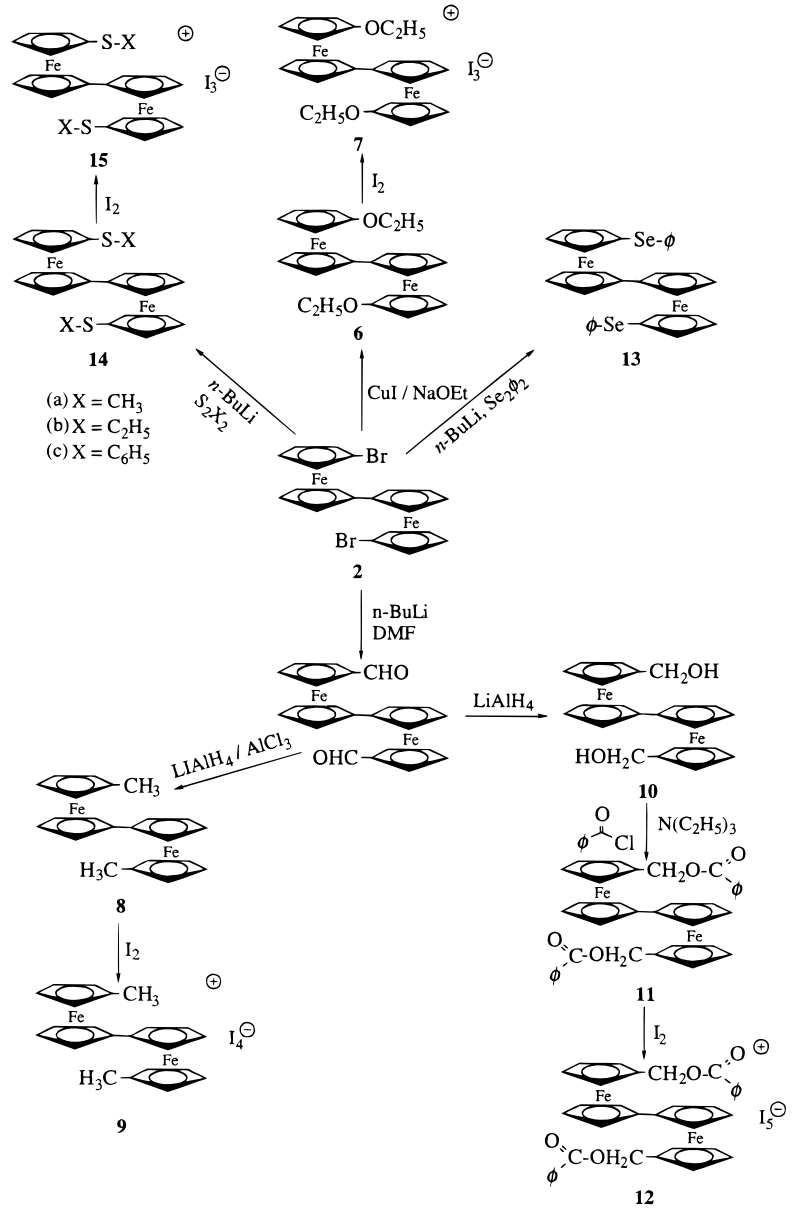

As illustrated in Table 3, a direct comparison of the average Fe−C, Fe−Cp ring, and Fe−fulvalenide (Fe−ful) ligand distances is made. Inspection of the average bond distance between the Fe atom and the five carbons (Fe−C) of a given Cp ring and the average Fe−Cp distance for a ferrocenyl moiety shows that these values are closer to the corresponding value observed for ferrocene[23] (2.045 Å for Fe−C and 1.65 Å for Fe−Cp) than the corresponding value observed for ferrocenium cation[24] (2.075 Å for Fe−C and 1.70 Å for Fe−Cp). The average C−C bond length in the Cp rings in these neutral compounds also agrees well with that in ferrocene (1.42 Å). In these compounds, the two least-

(23) Seiler, P.; Dunitz, J. D. *Acta Crystallogr., Sect. B* **1979**, *35*, 1068.
(24) Mammano, N. J.; Zalkin, A.; Landers, A.; Rheingold, A. L. *Inorg. Chem.* **1977**, *16*, 297.

Table 3. Comparison of the Atomic Distances (Å) and Angles (deg)

compd	Fe−C[a]	Fe−Cp[b]	Fe−ful[c]	ta[d]	da[e]	sa[f]
			Neutral Biferrocene			
biferrocene	2.052(3)	1.64(2)	1.65(2)	1.2	0	16
4	2.042(6)	1.647(3)	1.647(4)	1.4(3)	2.1(3)	2.1(4)
		1.646(3)	1.649(4)	1.7(3)		8.0(5)
6	2.043(4)	1.650(2)	1.650(2)	5.0(2)	3.9(2)	17.1(3)
		1.656(2)	1.647(2)	2.2(2)		8.6(3)
8	2.042(4)	1.651(4)	1.649(4)	3.3(2)	0	4.4(3)
10	2.044(4)	1.650(2)	1.650(2)	3.3(2)	1.6(2)	4.5(3)
		1.652(2)	1.652(2)	1.9(2)		15.2(3)
11	2.046(4)	1.649(2)	1.655(2)	1.8(2)	0	6.6(3)
14a	2.037(4)	1.643(5)	1.648(5)	1.5(5)	0	2.8(8)
14b	2.040(4)	1.642(4)	1.653(4)	1.9(2)	0	1.0(2)
			Mixed-Valence Biferrocenium			
7	2.061(5)	1.682(5)	1.665(5)	5.7(3)	0	2.7(3)
9	2.07(1)[g]	1.674(7)[g]	1.703(7)[g]	4.8(6)[g]	6.8(6)	1.7(7)[g]
	2.04(1)[h]	1.679(9)[h]	1.625(6)[h]	3.0(7)[h]		4.1(8)[h]
12	2.061(6)	1.675(5)	1.667(4)	2.5(4)	0	6.6(7)
15c	2.041(8)[g]	1.651(8)[g]	1.650(8)[g]	1.7(3)[g]	4.3(3)	2.1(3)[g]
	2.081(8)[h]	1.698(8)[h]	1.704(8)[h]	4.6(3)[h]		3.0(3)[h]

[a] Average Fe−C distance. [b] The distance between the Fe atom and the Cp ring. [c] The distance between the Fe and the fulvalenide ligand. [d] Dihedral angle between the Cp ring and the fulvalenide ligand. [e] Dihedral angle between the two Cp rings in the fulvalenide ligand. [f] Stagger angle between the Cp ring and the fulvalenide ligand. [g] Associated with Fe1. [h] Associated with Fe2.

Table 4. Experimental and Crystal Data for the X-ray Structures of Mixed-Valence Biferrocenium Triiodides

	7	**9**	**12**	**15c**
formula	$C_{24}H_{26}Fe_2I_3O_2$	$C_{22}H_{22}Fe_2I_4$	$C_{36}H_{30}Fe_2I_5O_4$	$C_{32}H_{26}Fe_2I_3S_2$
mol wt	838.84	905.72	1268.80	967.05
cryst syst	triclinic	monoclinic	triclinic	triclinic
space group	$P\bar{1}$	$C2$	$P\bar{1}$	$P\bar{1}$
a, Å	7.352(2)	15.010(2)	9.389(2)	10.641(2)
b, Å	9.495(2)	14.254(2)	11.168(2)	10.623(2)
c, Å	10.472(2)	13.715(4)	11.274(2)	16.690(2)
α, deg	112.02(1)		61.63(1)	89.78(1)
β, deg	99.92(1)	120.13(1)	76.28(1)	78.41(1)
γ, deg	100.27(2)		65.97(1)	60.23(1)
ρ_{calcd}, g cm^{-3}	2.165	2.370	2.228	2.015
V, Å^3	643.5(3)	2538.1(9)	948.6(3)	1594.0(5)
Z	1	4	1	2
μ, mm^{-1}	4.744	11.94	4.869	3.967
λ, Å	0.709 30	0.710 69	0.709 30	0.709 30
2θ limits, deg	44.86	44.9	44.86	44.94
R_f[a]	0.0243	0.025	0.0297	0.0364
R_{wf}[b]		0.024		
wR2[c]	0.061		0.0702	0.0986

[a] $R_f = \sum(||F_o| - |F_c||)/\sum|F_o|$. [b] $R_{wf} = \sum[(w(F_o - F_c)^2)/\sum(wF_o^2)]^{1/2}$. [c] $wR2 = [(\sum w(F_o^2 - F_c^2)^2)/(\sum wF_o^2)^2]^{1/2}$, where $w = 1/[\sigma^2(F_o^2) + (fp)^2]$, $p = (\max(F_o^2; 0) + 2F_c^2)/3$, and $f = 0.0340$ for **7**, 0.0363 for **12**, and 0.0499 for **15c**.

squares planes of the Cp rings for a given ferrocenyl moiety form a nearly parallel geometry, while these two Cp rings are nearly eclipsed (see the ta and sa values in Table 3).

Molecular Structures of Mixed-Valence Biferrocenium Salts (7, 9, 12, and 15c). The experimental and crystal data of the X-ray structures are collected in Table 4. Collected in Tables 5 and 6 are selected bond distances and angles. A direct comparison is also made between these mixed-valence biferrocenium salts and neutral biferrocenes (Table 3). Figures 2−5 show the molecular structures and atomic labeling schemes for the cation and anion. These mixed-valence compounds also exist in a trans conformation.

Table 5. Selected Bond Distances (Å) and Bond Angle (deg)

	7	**12**
	Bond Distances	
I1−I2	2.9255(7)	2.9129(8)
I3−I3[a]		2.749(1)
Fe−C1	2.082(5)	2.071(5)
Fe−C2	2.057(5)	2.047(5)
Fe−C3	2.049(5)	2.050(6)
Fe−C4	2.044(5)	2.062(7)
Fe−C5	2.039(5)	2.055(6)
Fe−C6	2.132(5)	2.072(6)
Fe−C7	2.066(5)	2.063(6)
Fe−C8	2.031(5)	2.057(6)
Fe−C9	2.030(5)	2.055(6)
Fe−C10	2.081(5)	2.074(6)
C1−C1[b]	1.47(1)	1.45(1)
C1−C2	1.428(7)	1.433(8)
C1−C5	1.410(7)	1.426(8)
C2−C3	1.408(7)	1.408(9)
C3−C4	1.421(8)	1.406(9)
C4−C5	1.403(7)	1.396(9)
C6−C7	1.414(7)	1.415(8)
C6−C10	1.414(7)	1.407(9)
C7−C8	1.415(8)	1.415(9)
C8−C9	1.402(8)	1.405(9)
C9−C10	1.415(8)	1.397(9)
	Bond Angles	
I2−I1−I2[c]	180.0	180.0
C1[b]−C1−C2	125.8(5)	126.5(7)
C1[b]−C1−C5	126.3(5)	126.8(7)
C2−C1−C5	107.5(4)	106.5(5)
C1−C2−C3	107.5(4)	107.9(5)
C2−C3−C4	108.6(5)	108.5(6)
C3−C4−C5	107.3(5)	108.3(6)
C1−C5−C4	109.1(4)	108.8(6)
C7−C6−C10	109.1(5)	107.8(5)
C6−C7−C8	106.5(5)	108.1(5)
C7−C8−C9	108.9(5)	107.1(6)
C8−C9−C10	108.3(5)	109.2(6)
C6−C10−C9	106.9(5)	107.9(5)

[a] Symmetry equivalents: $-x + 2, -y, -z + 1$ for **12**. [b] Symmetry equivalents: $-x + 2, -y + 1, -z + 1$ for **7**; $-x + 2, -y + 1, -z$ for **12**. [c] Symmetry equivalents: $-x, -y, -z$ for **7** and **12**.

In the case of **7** and **12**, the site symmetry imposed on the mixed-valence cation obviously requires that both iron centers of the cation are in equivalent positions. In **7** and **12**, the Fe−C distances are 2.061(5) and 2.061(6) Å, respectively. Each value is marginally larger than that for the corresponding neutral biferrocene compound. It lies midway between the 2.045 Å observed for ferrocene[23] and 2.075 Å observed for the ferrocenium cation.[24] The respective average Fe−Cp and Fe−ful distances in **7** and **12** are 1.674(5) and 1.671(5) Å, which are also larger than that for the corresponding neutral biferrocene. Such an increase in the Fe−C and Fe−Cp distances has been observed when ferrocenes are oxidized to the corresponding ferrocenium ion.[24] Furthermore, inspection of the Fe−Cp distances in **7** and **12** shows that these values also lie midway between the value of 1.65 Å found for ferrocene[23] and the value of 1.70 Å found for the ferrocenium ion.[24] The dihedral angles between the two least-squares Cp planes for a given ferrocenyl moiety in **7** and **12** are 5.7(3)° and 2.5(4)°, respectively. The two Cp rings in each ferrocenyl moiety in **7** and **12** are nearly eclipsed with average staggering angles of 2.7(3)° and 6.6(7)°, respectively.

In the case of mixed-valence cations **9** and **15c**, the two ferrocenyl moieties are not equivalent. In **9**, the Fe1−C distance (2.07(1) Å) and the average Fe1−Cp and Fe−ful distance (1.688 Å), which are larger than

Table 6. Selected Bond Distance (Å) and Bond Angles (deg)

	9	15c
	Bond Distances	
I1−I2	3.010(2)	2.9326(9)
I1−I3	2.850(2)	2.876(1)
I2−I4	3.394(2)	
I4−I4[a]	2.788(2)	
Fe1−C1	2.128(9)	2.038(7)
Fe1−C2	2.11(1)	2.046(8)
Fe1−C3	2.08(1)	2.044(8)
Fe1−C4	2.06(1)	2.033(7)
Fe1−C5	2.06(1)	2.033(7)
Fe1−C6	2.10(1)	2.024(8)
Fe1−C7	2.05(1)	2.035(8)
Fe1−C8	2.03(1)	2.053(7)
Fe1−C9	2.03(1)	2.039(8)
Fe1−C10	2.07(1)	2.050(8)
Fe2−C11	2.030(9)	2.136(7)
Fe2−C12	2.02(1)	2.089(8)
Fe2−C13	2.03(1)	2.071(8)
Fe2−C14	2.02(1)	2.057(8)
Fe2−C15	2.04(1)	2.072(8)
Fe2−C16	2.06(1)	2.142(8)
Fe2−C17	2.04(1)	2.064(9)
Fe2−C18	2.06(1)	2.043(8)
Fe2−C19	2.07(1)	2.053(8)
Fe2−C20	2.06(1)	2.086(8)
C1−C2	1.41(2)	1.44(1)
C1−C5	1.41(2)	1.41(1)
C1−C11	1.48(1)	1.45(1)
C2−C3	1.44(2)	1.39(1)
C3−C4	1.41(2)	1.43(1)
C4−C5	1.41(2)	1.39(1)
C6−C7	1.43(2)	1.41(1)
C6−C10	1.41(2)	1.43(1)
C7−C8	1.41(2)	1.40(1)
C8−C9	1.37(2)	1.40(1)
C9−C10	1.40(2)	1.41(1)
C11−C12	1.42(1)	1.41(1)
C11−C15	1.43(2)	1.43(1)
C12−C13	1.43(2)	1.42(1)
C13−C14	1.44(2)	1.40(1)
C14−C15	1.40(2)	1.40(1)
C16−C17	1.41(2)	1.41(1)
C16−C20	1.42(2)	1.42(1)
C17−C18	1.38(2)	1.39(1)
C18−C19	1.39(3)	1.40(1)
C19−C20	1.40(2)	1.40(1)
	Bond Angles	
I2−I1−I3	177.38(4)	175.05(3)
I1−I2−I4	96.15(3)	
I2−I4−I4[a]	176.08(5)	
C2−C1−C5	108.5(9)	107.6(7)
C2−C1−C11	124(1)	124.8(7)
C5−C1−C11	126(1)	127.6(7)
C1−C2−C3	108(1)	107.7(8)
C2−C3−C4	107(1)	108.2(7)
C3−C4−C5	109(1)	108.1(8)
C1−C5−C4	108(1)	108.4(8)
C7−C6−C10	107(1)	108.7(7)
C6−C7−C8	107(1)	107.4(8)
C7−C8−C9	109(1)	108.8(7)
C8−C9−C10	109(1)	109.2(7)
C6−C10−C9	108(1)	105.9(7)
C1−C11−C12	125(1)	126.0(7)
C1−C11−C15	124.5(9)	126.2(7)
C12−C11−C15	109.7(9)	107.3(7)
C11−C12−C13	107(1)	107.6(7)
C12−C13−C14	107(1)	108.7(7)
C13−C14−C15	109(1)	108.1(7)
C11−C15−C14	106(1)	108.2(7)
C17−C16−C20	107(1)	107.3(7)
C16−C17−C18	108(1)	108.6(8)
C17−C18−C19	110(1)	108.0(7)
C18−C19−C20	108(1)	108.5(7)
C16−C20−C19	108(1)	107.5(7)

[a] Symmetry equivalent: $1 - x, y, 2 - z$ for **9**.

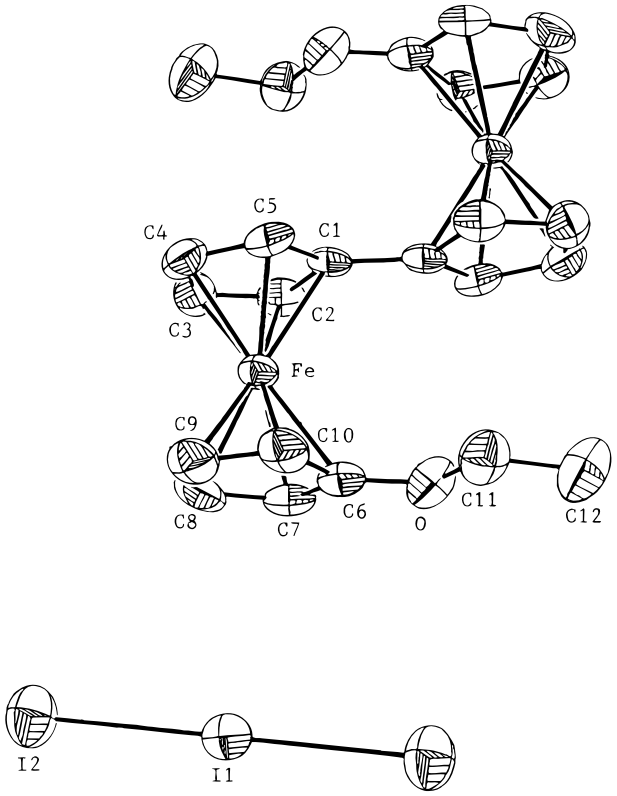

Figure 2. ORTEP drawing of mixed-valence **7**.

the corresponding values in ferrocene and neutral biferrocene **8**, indicate that the Fe1$(Cp)_2$ metallocene unit is in the Fe(III) oxidation state. However, in comparison with ferrocene and the corresponding neutral biferrocene **8**, the Fe2−C distance (2.04(1) Å) and the average Fe2−Cp and Fe−ful distance (1.652(8) Å) indicate that the Fe2$(Cp)_2$ metallocene unit is in the Fe(II) oxidation state. Similarly, making a comparison of the Fe−C and Fe−Cp distances in **15c** indicates that Fe1 is in the Fe(II) oxidation state and Fe2 is in Fe(III) oxidation state.

In **9** and **15c**, the two Cp units in the fulvalenide moiety are not crystallographically coplanar and the dihedral angles between the two Cp units are 6.8(6)° and 4.3(3)°, respectively. In both compounds (**9** and **15c**), the two least-squares planes of the Cp rings for a given ferrocenyl moiety form a nearly parallel geometry while the two Cp rings are nearly eclipsed.

The triiodide anions in **7** and **12** are linear, and they also show a symmetric structure. The I1−I2 distances in **7** and **12** are 2.9255(7) and 2.9129(8) Å, respectively. The solid-state structures of **7** and **12** are composed of columns of biferrocenium cations and triiodide anions. However, in **12**, the polyiodide ions contain zigzag chains of alternate I_3^- and I_2 units. This well-established polyiodide chain is also seen in structurally characterized mixed-valence 1′,1‴-bis(*p*-bromobenzyl)-biferrocenium pentaiodide.[25] This type of arrangement, alternating I_3^- and I_2, is quite common among the pentaiodide salts. In **12**, the bond length in the I_2 molecule is 2.749(1) Å, significantly larger than the value of 2.68 Å found in crystalline I_2.[26]

(25) Dong, T.-Y.; Schei, C. C.; Hwang, M. Y.; Lee, T. Y.; Yeh, S. K.; Wen, Y. S. *Organometallics* **1992**, *11*, 573.

(26) Kitaigorodskii, A. I.; Khotsyanova, T. L.; Struchkov, Y. T. *Zh. Fiz. Khim.* **1953**, *27*, 780.

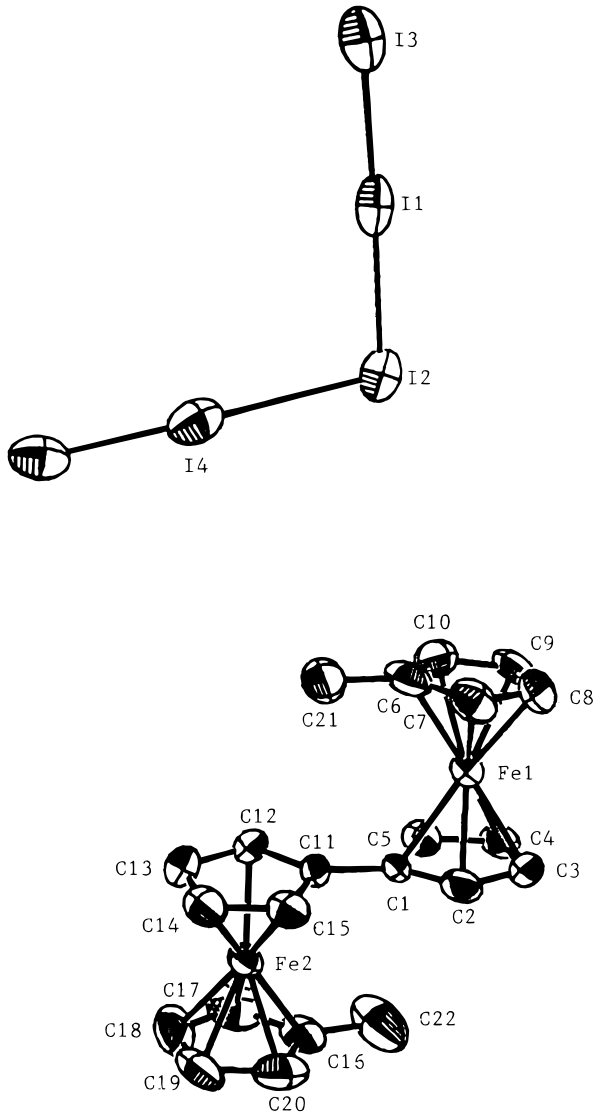

Figure 3. ORTEP drawing of mixed-valence **9**.

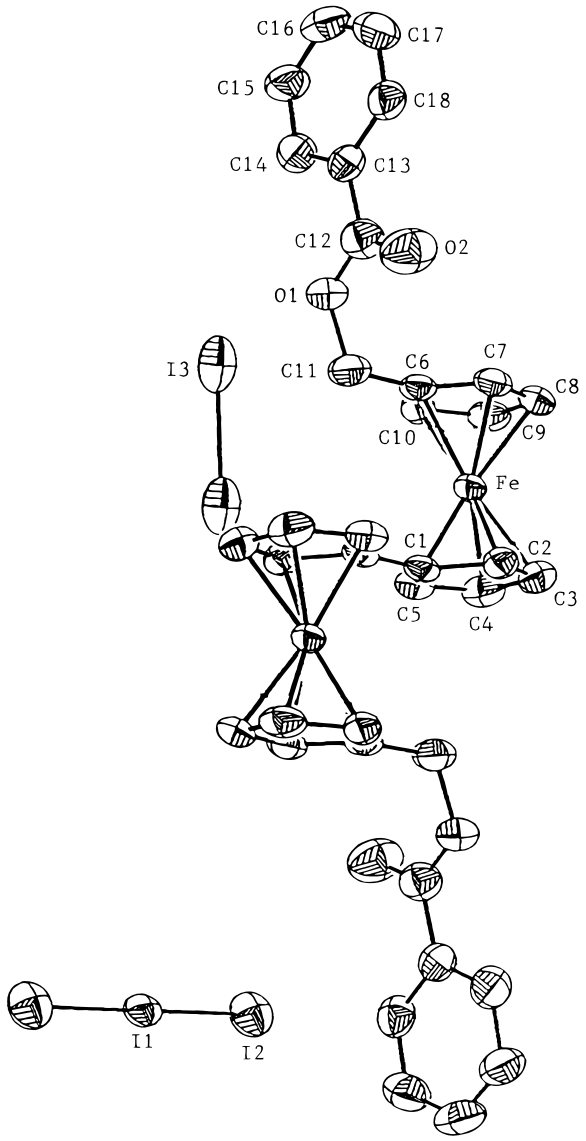

Figure 4. ORTEP drawing of mixed-valence **12**.

On the other hand, the triiodide anions in **9** and **15c** are essentially linear, and the I2−I1−I3 angles are 177.38(4)° and 175.05(3)°, respectively. However, the triiodide anions in **9** and **15c** have an asymmetric structure with distances of I1−I2 = 3.010(2) and 2.9226(9) Å and I1−I3 = 2.850(2) and 2.876(1) Å, respectively. In other words, the triiodide anion possesses I_2-I^- character, where the I2 atom carries more negative charge than the other terminal I3 atom. In **9**, the polyiodide ions also contain zigzag chains of alternating I_3^- and I_2 units. The bond length in the I_2 molecule is 2.788(2) Å. The distance between neighboring iodine atoms in I_2 and I_3^- units (I2−I4 = 3.394(2) Å) within a chain indicates a significant interaction, in view of the in-plane intermolecular distance of 3.50 Å found in crystalline I_2.[26]

Electrochemical Measurements. Electrochemical data for the neutral biferrocenes **4**, **6**, **8**, **10**, **11**, and **14**, as well as those for some other relevant compounds, are shown in Table 7. These binuclear biferrocenes all undergo two successive reversible one-electron oxidations to yield the mono- and then the dication. Electrochemical reversibility is demonstrated by the peak-to-peak separation between the resolved reduction and oxidation wave maxima (Δ in Table 7) and a 1:1 relationship of the cathodic and anodic peak currents (I_c/I_a in Table 7).

The effect of the substituent on the stability of the ferrocenium cation is illustrated by the shift of the half-wave potential ($E_{1/2}$). The electron-donating groups ($-CH_2OCH_3$, $-OC_2H_5$, $-CH_2OH$, $-SCH_3$, and $-SC_2H_5$) stabilize the cation, lowering the half-wave potential, while the electron-withdrawing groups ($-CH_2OCOC_6H_5$ and $-SC_6H_5$) have the opposite effect.

From the value of $\Delta E_{1/2}$, the disproportionation equilibrium constant K (eq 1) can be calculated. In eq 1,

$$[2,2] + [3,3] \overset{K}{\rightleftharpoons} 2[2,3] \qquad (1)$$

the abbreviations [3,3], [2,3], and [2,2] denote the dioxidized salt, the monooxidized salt, and the neutral compound, respectively. The large value of K gives an indication of the possibility of preparing the mixed-valence biferrocenium salts. Except for the neutral biferrocenes **10** and **13**, mixed-valence compounds **5**, **7**, **9**, **12**, and **15** were prepared by oxidizing the corresponding neutral biferrocenes with I_2. The resulting microcrystalline samples were recrystallized from a

(27) Nakashima, S.; Katada, M.; Motoyama, I.; Sano, H. *Bull. Chem. Soc. Jpn.* **1987**, *60*, 2253.

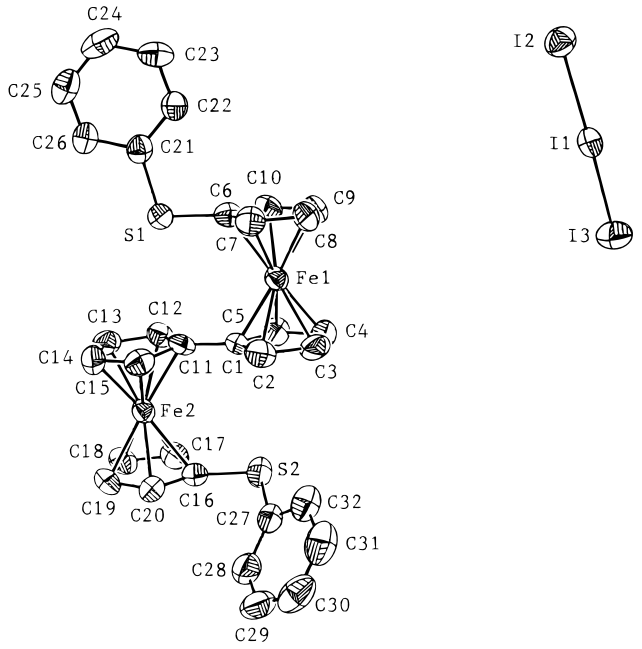

Figure 5. ORTEP drawing of mixed-valence **15c**.

Table 7. Cyclic Voltammetry for Various Biferrocenes

compd	$E_{1/2}$,[a] V	$\Delta E_{1/2}$,[b] V	Δ,[c] mV	I_c/I_a[d]	K ($\times 10^{-5}$)
ferrocene	0.37		70	0.97	
biferrocene	0.28	0.31	70	1.01	1.8
	0.59		75	1.01	
4	0.29	0.32	70	0.87	2.6
	0.61		72	1.08	
6	0.13	0.34	79	0.96	5.8
	0.47		70	1.03	
10	0.26	0.31	61	0.89	1.8
	0.57		60	1.01	
11	0.35	0.32	73	0.81	2.6
	0.68		75	0.98	
13	0.38	0.28	73	0.86	0.6
	0.66		73	1.03	
14a	0.26	0.30	64	0.88	1.2
	0.56		69	1.04	
14b	0.27	0.30	75	0.86	1.2
	0.57		65	1.06	
14c	0.37	0.28	70	0.83	0.6
	0.65		71	1.00	

[a] All half-wave potentials are referred to the Ag^+/Ag electrode. [b] Peak separation between waves. [c] Peak-to-peak separation between the resolved reduction and oxidation wave maxima. [d] Peak current ratio between cathode and anode.

CH_2Cl_2/hexane solution. The physical properties for this series of new mixed-valence salts are described in next section.

Electron Transfer in the Solid State. The rates of intramolecular electron transfer in the solid state of the mixed-valence cations **5**, **7**, **9**, **12**, and **15** were estimated by variable-temperature ^{57}Fe Mössbauer spectroscopy (time scale $\sim 10^7$ s^{-1}). Typical ^{57}Fe Mössbauer spectra of **5** are given in Figure 6. The various absorption peaks in the Mössbauer spectra of these compounds were fitted to Lorentzian lines. The resulting fitting parameters are collected in Table 8.

The rates of electron transfer in mixed-valence cations **5**, **7**, **9**, **12**, and **15** can be sensitively controlled by the substituents. In this new series of mixed-valence cations, three basic types of biferrocenium salts are found. The cations of **9**, **12**, and **15c** have localized electronic structures at temperatures below 300 K

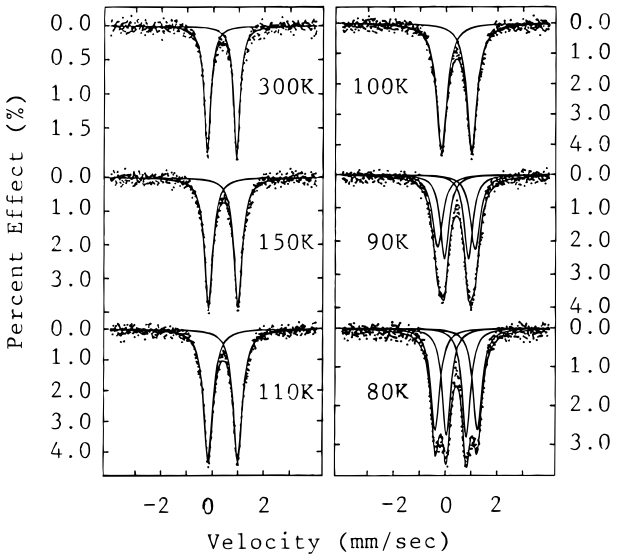

Figure 6. Variable-temperature ^{57}Fe Mössbauer spectra of **5**.

Table 8. Variable-Temperature ^{57}Fe Mössbauer Least-Squares-Fitting Parameters

compd	T, K	ΔE_Q[a]	δ[b]	Γ[c]
5	300	1.151	0.448	0.301, 0.313
	150	1.160	0.507	0.389, 0.391
	130	1.159	0.514	0.405, 0.403
	110	1.160	0.518	0.438, 0.436
	100	1.168	0.521	0.481, 0.483
	90	1.457	0.516	0.465, 0.480
		0.935	0.522	0.412, 0.412
	80	1.633	0.524	0.422, 0.422
		0.776	0.528	0.394, 0.403
7	300	1.177	0.447	0.338, 0.342
	80	1.214	0.523	0.461. 0.458
9	300	1.737	0.443	0.301, 0.308
		0.583	0.436	0.277, 0.278
	80	1.882	0.515	0.288, 0.287
		0.416	0.519	0.282, 0.283
12	300	1.333	0.447	0.518, 0.474
		0.737	0.454	0.596, 0.520
	80	1.958	0.515	0.347, 0.353
		0.453	0.512	0.506, 0.434
15a	300	1.218	0.453	0.299, 0.284
	80	1.263	0.526	0.334, 0.320
15b	300	1.188	0.457	0.383, 0.372
	80	1.249	0.526	0.513, 0.501
15c	300	2.105	0.442	0.247, 0.264
		0.625	0.455	0.310, 0.270
	80	2.122	0.514	0.247, 0.246
		0.625	0.535	0.291, 0.287

[a] Quadrupole-splitting in mms^{-1}. [b] Isomer shift referenced to iron-foil in mms^{-1}. [c] Full width at half-height taken from the least-squares-fitting program. The width for the line at a more positive velocity is listed first for each doublet.

(electron-transfer rate $< \sim 10^7$ s^{-1}). On the other hand, compounds **7**, **15a**, and **15b** have delocalized electronic structures (electron-transfer rate $> \sim 10^7$ s^{-1}) between 80 and 300 K. Compound **5** gives temperature-dependent Mössbauer spectra (Figure 6).

In the case of **9**, **12**, and **15c**, the features in all of the 300 and 80 K spectra include two doublets, one with a quadrupole splitting (ΔE_Q) ~ 2 mm s^{-1} (Fe(II) site) and the other with $\Delta E_Q = \sim 0.5$ mm s^{-1} (Fe(III) site). Both doublets are fitted into a 1:1 area ratio. This pattern of two doublets is expected for a biferrocenium cation which is valence-trapped on the time scale of the Mössbauer experiment (electron-transfer rate $< \sim 10^7$ s^{-1}).[8] Furthermore, in **12**, the Mössbauer behavior is

different from what is seen for **9** and **15c**. The two doublets, $\Delta E_Q = 1.333$ and 0.737 mm s^{-1} at 300 K, just move together. We believe that the decrease of ΔE_Q in the ferrocenyl doublet and the increase of ΔE_Q in the ferrocenium doublet are related to the magnitude of electron-transfer rate in the cation. Thus, the rate of electron transfer in **12** is greater than that in **9** or **15c**. It should be noted that the electron-transfer rate in mixed-valence 1′,1‴-dimethylbiferrocenium triiodide was reported before.[27] Sano et al. were able to prepare a triiodide (I_3^-) salt of the mixed-valence cation of 1′,1‴-dimethylbiferrocenium. In our hands, attempts to prepare a triiodide salt of the mixed-valence cation by use of stoichiometric amounts of iodine resulted in a I_4^- salt (**9**). The Mössbauer spectrum of their compound, taken at 298 K, also shows two quadrupole-split doublets ($\Delta E_Q = 1.74$ and 0.56 mm s^{-1}).

The Mössbauer results indicate that compounds **7**, **15a**, and **15b** are delocalized on the Mössbauer time scale above 80 K. Only a single "average-valence" doublet ($\Delta E_Q = \sim 1.2$ mm s^{-1}) in each Mössbauer spectrum is seen from 80 to 300 K.

In the case of **5**, at temperatures below 90 K, there are two doublets in each Mössbauer spectrum, one representing the Fe(II) site and the other Fe(III) site. An increase of temperature causes the two doublets to move together, resulting in an "average-valence" doublet at 100 K. At temperatures above 100 K, the spectrum shows only a single quadrupole-split doublet which is characteristic of a valence-detrapped cation (electron-transfer rate > $\sim 10^7$ s^{-1}).

IR spectroscopy has also been applied to study the rate of electron transfer. It has been shown that the perpendicular C−H bending band is the best diagnosis of the Fe oxidation state. This band is seen at 815 cm^{-1} for ferrocene and at 850 cm^{-1} for ferrocenium triiodide.[8] A localized mixed-valence biferrocenium cation should exhibit one C−H bending band for the Fe(II) ferrocenyl moiety and one for the Fe(III) ferrocenium moiety.[8]

Infrared spectra were run on KBr pellets of the series of biferrocenium cations. For **5**, **7**, **9**, **12**, and **15**, there are relatively strong bands at ∼818 and ∼840 cm^{-1} in the perpendicular C−H bending region. It is clear that the IR data conclusively indicate the presence of Fe(II) and Fe(III) moieties.

Experimental Section

General Information. All manipulations involving air-sensitive materials were carried out by using standard Schlenk techniques under an atmosphere of N_2. Chromatography was performed on neutral alumina (Merck, activity II). Solvents were dried as follows: benzene, hexane, ether, and THF distilled from Na/benzophenone; CH_2Cl_2 and $(CH_3)_2S_2$ distilled from CaH_2. 1,1′-Dibromoferrocene was prepared according to the literature procedure.[21]

1′,1‴-Dibromobiferrocene (2). Dibromoferrocene (34.4 g, 0.11 mol) was placed in a freshly oven-dried three-necked flask (500 mL) and dried under vacuum at 2 mmHg at 25 °C for 4 h. Dried THF (250 mL), followed by *n*-butyllithium (0.1 mol), was added under nitrogen. The resulting solution was stirred at −30 °C for 30 min, during which 1-bromo-1′-lithioferrocene gradually precipitated. Solid CuCN (4.5 g, 50 mmol) was then added, and the solution was stirred further at −30 °C for 10 min. At −78 °C, oxygen was bubbled continuously through the solution for 4 h. The solution was then stirred at room temperature for another 4 h. Water (200 mL) was added, and the mixture was then extracted with CH_2Cl_2. The combined extracts were dried over $MgSO_4$ and evaporated at reduced pressure. The residue was recrystallized from methanol in a refrigerator overnight (yield 45%). The compound thus prepared is pure (identification with NMR and melting point)[22] and can be used for further reaction. Further purification could be carried out by chromatography, if necessary.

1′-(Methoxymethyl)-1-bromoferrocene (3). At −30 °C, *n*-BuLi (10 mmol) was added under nitrogen into a THF (40 mL) solution of dibromoferrocene (3.44 g, 10 mmol) and the resulting solution was stirred for 30 min. Electrophilic reagent ICH_2OCH_3 (10 mmol) was then added, and the solution was further stirred at −30 °C for another 30 min. Water (40 mL) was added, and the resulting mixture was extracted with ether (40 mL × 2). The combined extracts were dried over $MgSO_4$ and evaporated at reduced pressure. The residue was chromatographed on Al_2O_3. The first band eluted with hexane was the starting material containing some impurities. Continued elution with hexane:CH_2Cl_2 (4:1) gave elutes which yielded the desired compound (69% yield). The properties of **3** are as follows. ^{1}H NMR ($CDCl_3$, ppm): 3.30 (s, 3H, $-CH_3$), 4.04 (t, 2H, Cp), 4.10 (s, 2H, $-CH_2$), 4.19 (s, 4H, Cp), 4.34 (t, 2H, Cp). MS: M^+ at *m*/*z* 308 and 310.

1′,1‴-Bis(methoxymethyl)biferrocene (4). Compound **3** (2 mmol) was thoroughly mixed with activated Cu (5 g), and the resulting mixture was heated at 120 °C (oil bath) for 22 h. The solid was cooled to room temperature and then subjected to the Soxhlet process with dichloromethane. The extract was evaporated at reduced pressure, and the residue was chromatographed on Al_2O_3. Elution with hexane gave elutes containing starting material and ferrocene. Continued elution with dichloromethane:hexane (1:4) gave the desired biferrocenes **4** (63% yield). ^{1}H NMR ($CDCl_3$, ppm): 3.21 (s, 6H, $-CH_3$), 3.96 (s, 4H, Cp), 3.98 (d, 4H, Cp), 4.01 (d, 4H, Cp), 4.17 (t, 4H, Cp), 4.30 (t, 4H, Cp). MS: M^+ at *m*/*z* 458. Mp: 101−102 °C.

1′,1‴-Bis(ethoxyl)biferrocene (6). Cuprous iodide (0.19 g, 1.0 mmol) and sodium ethoxide (0.272 g, 4.0 mmol) were added under nitrogen into a 8 mL ethanol/DMF (3:5) solution of dibromobiferrocene (0.528 g, 1.27 mmol). The resulting solution was refluxed for 75 min. Water (10 mL) was added, and the resulting mixture was extracted with CH_2Cl_2 (20 mL × 3). The combined extracts were dried over $MgSO_4$ and evaporated at reduced pressure. The residue was chromatographed on Al_2O_3 (activity III). Elution with hexane gave elutes containing some impurities, which were discarded. Continued elution with CH_2Cl_2:hexane (1:5) gave monosubstituted 1′-ethoxylbiferrocene (15% yield). The third band was the desired compound **6** (21% yield). The physical properties of 1′-ethoxylbiferrocene are as follows. ^{1}H NMR ($CDCl_3$, ppm): 1.22 (t, 3H, $-CH_3$), 3.68 (m, 4H, $-CH_2-$ and Cp), 3.94 (t, 2H, Cp), 4.01 (s, 5H, Cp), 4.20 (dt, 4H, Cp), 4.35 (t, 4H, Cp). MS: M^+ at *m*/*z* 414. Mp: 124.0−124.3 °C. The physical properties of **6** are as follows. ^{1}H NMR ($CDCl_3$, ppm): 1.23 (t, 6H, $-CH_3$), 3.66 (m, 8H, $-CH_2-$ and Cp), 3.90 (d, 4H, Cp), 4.20 (t, 4H, Cp), 4.39 (t, 4H, Cp). MS: M^+ at *m*/*z* 458. Mp: 104.9−105.2 °C.

General Procedure of 1′,1‴-Disubstituted Biferrocenes. At −30 °C, 7.6 mL of *n*-BuLi (1.3 M in hexane) was added under nitrogen to a THF (40 mL) solution of dibromobiferrocene (2.64 g, 5.0 mmol). The resulting solution was stirred at −30 °C for 30 min. Various electrophilic reagents (10 mmol) were then added, and the solution was stirred further at −30 °C for another 30 min. Water (40 mL) was added, and the resulting mixture was extracted with CH_2Cl_2. The combined extracts were dried over $MgSO_4$ and evaporated at reduced pressure. The residue was chromatographed on Al_2O_3. Elution with hexane:CH_2Cl_2 (5:1) gave the disubstituted biferrocenes.

1′,1‴-Bis(carbaldehyde)biferrocene (1.598 g, 75% yield) was obtained with DMF (1 mL) as the electrophilic reagent. ^{1}H

NMR ($CDCl_3$, ppm): 4.33 (d, 4H, Cp), 4.41 (d, 4H, Cp), 4.45 (d, 4H, Cp), 4.60 (d, 4H, Cp), 9.73 (s, 2H, −CHO). MS: M^+ at m/z 426.

1′,1‴-Bis(phenylseleno)biferrocene (**13**, 47% yield) was obtained with $(C_6H_5)_2Se_2$ as the electrophilic reagent. ^1H NMR ($CDCl_3$, ppm): 4.14 (t, 4H, Cp), 4.20 (t, 4H, Cp), 4.30 (t, 4H, Cp), 4.48 (t, 4H, Cp), 7.17 (m, 10H, $-C_6H_5$). MS: M^+ at m/z 682. Mp: 190.9−191.8 °C.

1′,1‴-Bis(methylthio)biferrocene (**14a**, 24% yield) was obtained with $(CH_3)_2S_2$ as the electrophilic reagent. ^1H NMR ($CDCl_3$, ppm): 2.23 (s, 6H, $-CH_3$), 4.02 (t, 4H, Cp), 4.11 (t, 4H, Cp), 4.25 (t, 4H, Cp), 4.42 (t, 4H, Cp). MS: M^+ at m/z 462. Mp: 79.1−80.1 °C.

1′,1‴-Bis(ethylthio)biferrocene (**14b**, 47% yield) was obtained with $(C_2H_5)_2S_2$ as the electrophilic reagent. ^1H NMR ($CDCl_3$, ppm): 1.14 (s, 6H, $-CH_3$), 2.64 (q, 4H, $-CH_2-$), 4.09 (t, 4H, Cp), 4.20 (t, 4H, Cp), 4.30 (t, 4H, Cp), 4.49 (t, 4H, Cp). MS: M^+ at m/z 490. Mp: 69.3−70.5 °C.

1′,1‴-Bis(phenylthio)biferrocene (**14c**, 65% yield) was obtained with $(C_6H_5)_2S_2$ as the electrophilic reagent. ^1H NMR ($CDCl_3$, ppm): 4.18 (t, 8H, Cp), 4.31 (t, 4H, Cp), 4.50 (t, 4H, Cp), 7.03 (t, 6H, *p*- and *m*-benzyl), 7.15 (t, 4H, *o*-benzyl). MS: M^+ at m/z 586. Mp: 191 °C (dec).

1′,1‴-Dimethylbiferrocene (8). The reduction reaction was carried out by carefully adding, with stirring, a small portion of $AlCl_3$ to a mixture of 1′,1‴-bis(carbaldehyde)-biferrocene and $LiAlH_4$ in dry ether. After 30 min, the solution became yellow, an excess of H_2O was added to it, and the ether layer was separated. The ether layer was washed with H_2O and dried over $MgSO_4$. After evaporation of the solvent, the crude product was chromatographed on Al_2O_3, eluting with hexane. The first band was the desired compound (95% yield). ^1H NMR ($CDCl_3$, ppm): 1.75 (s, 6H, $-CH_3$), 3.85 (s, 4H, Cp), 3.88 (s, 4H, Cp), 4.13 (d, 4H, Cp), 4.26 (d, 4H, Cp). MS: M^+ at m/z 398. Mp: 149−150 °C.

1′,1‴-Bis(hydoxymethyl)biferrocene (10). The reduction reaction of 1′,1‴-bis(carbaldehyde)biferrocene was carried out according the same procedure described above, except using $LiAlH_4$ as the reducing reagent. Purification was carried out by recrystallizing from CH_2Cl_2. ^1H NMR ($CDCl_3$, ppm): 1.25 (s, 2H, −OH), 4.03 (d, 4H, Cp), 4.07 (d, 4H, Cp), 4.10 (d, 4H, $-CH_2-$), 4.27 (d, 4H, Cp), 4.40 (d, 4H, Cp). MS: M^+ at m/z 430. Mp: 148−149.5 °C.

1′,1‴-Bis(benzoyloxymethyl)biferrocene (11). To a 20 mL THF solution of **10** (0.1 g, 0.23 mmol) was added benzoyl chloride (0.5 mmol). The resulting solution was stirred 1 min, and then triethylamine was added. The mixture was placed in a refrigerator overnight. The solution was extracted with CH_2Cl_2 (20 mL × 3). The combined extracts were washed with H_2O, dried over $MgSO_4$, and evaporated at reduced pressure. The residue was chromatographed on Al_2O_3. Elution with hexane:CH_2Cl_2 (1:2) gave the desired compound. ^1H NMR ($CDCl_3$, ppm): 4.03 (t, 4H, Cp), 4.15 (t, 4H, Cp), 4.23 (t, 4H, Cp), 4.39 (t, 4H, Cp), 4.87 (s, 4H, $-CH_2-$), 7.40 (t, 4H, *m*-benzyl), 7.52 (td, 2H, *p*-benzyl), 7.99 (s, 4H, *o*-benzyl). MS: M^+ at m/z 638. Mp: 159 °C (dec).

Mixed-Valence Compounds 5, 7, 9, 12, and 15. Samples of these mixed-valence compounds were prepared by adding a benzene/hexane (1:1) solution containing a stoichiometric amount of iodine to a solution of the corresponding biferrocene at 0 °C. The corresponding biferrocene solution was prepared by dissolving the biferrocene in a proper solvent (benzene/hexane (1:1) for **4**, **6**, **8**, and **11**; hexane for **14a** and **14b**; CH_2Cl_2 for **14c**). The resulting dark crystals were filtered and washed repeatedly with cold hexane. Anal. Calcd for **5** ($C_{24}H_{26}Fe_2I_3O_2$): C, 34.36; H, 3.12. Found: C, 33.79; H, 3.06. Anal. Calcd for **7** ($C_{24}H_{26}Fe_2I_3O_3$): C, 34.36; H, 3.12. Found: C, 34.21; H, 3.14. Anal. Calcd for **9** ($C_{22}H_{22}Fe_2I_4$): C, 29.17; H, 2.45. Found: C, 28.84; H, 2.49. Anal. Calcd for **12** ($C_{36}H_{30}Fe_2I_5O_4$): C, 33.97; H, 2.38. Found: C, 33.74; H, 2.50. Anal. Calcd for **15a** ($C_{22}H_{22}Fe_2I_3S_2$): C, 31.35; H, 2.63. Found: C, 31.02; H, 2.64. Anal. Calcd for **15b** ($C_{24}H_{26}Fe_2I_{7/2}$): C, 30.85; H, 2.80. Found: C, 31.48; H, 2.93. Anal. Calcd for **15c** ($C_{32}H_{26}Fe_2I_3S_2$): C, 39.74; H, 2.71. Found: C, 38.80; H, 2.71.

Physical Methods. ^{57}Fe Mössbauer measurements were made on a constant-velocity instrument which was previously described.[28] Velocity calibration was made using a 99.99% pure 10-μm iron foil. Typical line widths for all three pairs of iron foil lines fell in the range 0.24−0.27 mm s^{-1}. Isomer shifts are reported relative to iron foil at 300 K but are uncorrected for temperature-dependent (second-order) Doppler effects. It should be noted that the isomer shifts illustrated in the figures are plotted as experimentally obtained. Tabulated data is provided.

^1H NMR spectra were run on a Varian VXR-300 spectrometer. Mass spectra were obtained with a VG-BLOTECH-QUATTRO 5022 system.

Electrochemical measurements were carried out with a BAS 100W system. Cyclic voltammetry was perform with a stationary glassy carbon working electrode, which was cleaned after each run. These experiments were carried out with a 1 × 10^{-3} M solution of biferrocene in dry CH_2Cl_2/CH_3CN (1:1) containing 0.1 M $(n\text{-}C_4H_9)_4NPF_6$ as the supporting electrolyte. The potentials quoted in this work are relative to a Ag/AgCl electrode at 25 °C. Under these conditions, ferrocene shows a reversible one-electron oxidation wave ($E_{1/2}$ = 0.37 V).

The single-crystal X-ray determinations of the compounds were carried out on an Enraf-Nonius CAD4 diffractometer at 298 K. Absorption corrections were made with empirical ψ rotation. A three-dimensional Patterson synthesis was used to determine the heavy-atom positions, which phased the data sufficiently well to permit location of the remaining non-hydrogen atoms from Fourier synthesis. All non-hydrogen atoms were refined anisotropically. Hydrogen atoms were calculated at ideal distances. The X-ray crystal data are summarized in Tables 1, 2, and 4. Selected bond distances and angles are given in Tables 5 and 6. Listings of the final positional parameters for all atoms, and thermal parameters of these compounds are given in the Supporting Information.

Structure Determination of 4. An orange crystal (0.1 × 0.15 × 0.35 mm) was obtained when a layer of hexane was allowed to slowly diffuse into a CH_2Cl_2 solution of **4**. Cell dimensions were obtained from 25 reflections with 17.78° < 2θ < 27.88°. The $\theta-2\theta$ scan technique was used to record the intensities for all reflections for which 1° < 2θ < 49.9°. Of the 2030 unique reflections, there were 1598 reflections with $F_o > 2.0\sigma(F_o^2)$, where $\sigma(F_o^2)$ was estimated from counting statistics.

Structure Determination of 6. An orange crystal (0.31 × 0.10 × 0.22 mm) was obtained following the same procedure as described for **4**. Data were collected to a 2θ value of 44.9°. The unit cell dimensions were obtained from 25 reflections with 14.98° < 2θ < 30.54°. Of the 2636 unique reflections, there were 1972 with $F_o > 2.5\sigma(F_o^2)$.

Structure Determination of 8. An orange crystal (0.16 × 0.20 × 0.22 mm) was obtained following the same procedure as described for **4**. The unit cell dimensions were obtained from 25 reflections with 23.8° < 2θ < 33.9°. Of the 1783 unique reflections, there were 1424 with $F_o > 3.0\sigma(F_o^2)$.

Structure Determination of 10. An orange crystal (0.31 × 0.28 × 0.19 mm) was obtained following the same procedure as described for **4**. The unit cell dimensions were obtained from 20 reflections with 15.06° < 2θ < 34.10°. Of the 2293 unique reflections, there were 1718 with $F_o > 2.5\sigma(F_o^2)$.

Structure Determination of 11. An orange crystal (0.13 × 0.64 × 0.32 mm) was obtained following the same procedure as described for **4**. Data were collected to a 2θ value of 44.9°. The cell dimensions were obtained from 25 reflections with 2θ in the range 11.72−28.69°. Of the 1819 unique reflections, there were 1405 with $F_o > 2.5\sigma(F_o^2)$.

(28) Dong, T.-Y.; Huang, C. H.; Chang, C. K.; Wen, Y. S.; Lee, S. L.; Chen, J. A.; Yeh, W. Y.; Yeh, A. *J. Am. Chem. Soc.* **1993**, *115*, 6357.

Structure Determination of 14a. An orange crystal (0.26 × 0.20 × 0.20 mm) was obtained by slow evaporation from a hexane solution of **14a**. Data were collected to a 2θ value of 44.98°. The cell dimensions were obtained from 25 reflections with 2θ in the range 19−27°. Of the 1362 unique reflections, there were 1265 with $F_o > 2.0\sigma(F_o^2)$.

Structure Determination of 14b. An orange crystal (0.36 × 0.28 × 0.26 mm) was obtained following the same procedure as described for **14a**. Data were collected to a 2θ value of 44.86°. The cell dimensions were obtained from 25 reflections with 2θ in the range 20−32°. Of the 2843 unique reflections, there were 2550 with $F_o > 2.0\sigma(F_o^2)$.

Structure Determination of 7. A dark black crystal (0.32 × 0.24 × 0.20 mm) was obtained following the same procedure as described for **4**. Data were collected to a 2θ value of 44.86°. The cell dimensions were obtained from 25 reflections with 2θ in the range 12−23°. Of the 1674 unique reflections, there were 1336 with $F_o > 2.0\sigma(F_o^2)$.

Structure Determination of 9. A dark black crystal (0.25 × 0.25 × 0.25 mm) was obtained following the same procedure as described for **4**. Data were collected to a 2θ value of 44.9°. The cell dimensions were obtained from 25 reflections with 2θ in the range 14.56−30.84°. Of the 1737 unique reflections, there were 1555 with $F_o > 2.0\sigma(F_o^2)$.

Structure Determination of 12. A dark black crystal (0.24 × 0.20 × 0.20 mm) was obtained following the same procedure as described for **4**. Data were collected to a 2θ value of 44.86°. The cell dimensions were obtained from 25 reflections with 2θ in the range 16−25°. Of the 2457 unique reflections, there were 1842 with $F_o > 2.0\sigma(F_o^2)$.

Structure Determination of 15c. A dark black crystal (0.22 × 0.18 × 0.16 mm) was obtained following the same procedure as described for **4**. Data were collected to a 2θ value of 44.94°. The cell dimensions were obtained from 25 reflections with 2θ in the range 11−21°. The data were also corrected for absorption. Of the 4181 unique reflections, there were 2717 with $F_o > 2.0\sigma(F_o^2)$.

Acknowledgments are made to the National Science Council (Grant No. NSC87-2113-M-110-010), Taiwan, ROC, and Department of Chemistry at Sun Yat-Sen University.

Supporting Information Available: Tables of positional parameters, bond distances and angles, and thermal parameters for **4**, **6**−**12**, **14a**, **14b**, and **15c**, ORTEP drawings for **4**, **6**, **8**, **10**, **11**, **14a**, and **14b**, and packing arrangements of **7**, **9**, **12**, and **15c** (44 pages). Ordering information is given on any current masthead page.

OM970746E